JOURNAL OF AIRCRAFT
Vol. 30, No. 5, Sept.–Oct. 1993

Response of B-2 Aircraft to Nonuniform Spanwise Turbulence

John P. Crimaldi,* Robert T. Britt,† and William P. Rodden‡
Northrop Corporation B-2 Division, Pico Rivera, California 90660

Design load requirements for random gusts prescribe a one-dimensional gust field, i.e., a field that is uniform spanwise for a vertical gust. By definition, such a gust will produce purely symmetric vehicle response with corresponding symmetric stresses. The more general case of a three-dimensional gust will cause an asymmetric response. The difference in response characteristics which may result are exemplified by the fact that at the centerline of a flying wing, symmetric shear and torsion are zero, whereas, the asymmetric values are not. Solution techniques based on cross-spectral methods have been applied to the B-2 aircraft to assess the nonuniform spanwise gust response characteristics. Results are presented comparing key vehicle response parameters for uniform and nonuniform gust loading. It is concluded that the uniform gust model generally produces the higher loads and that no additional design conditions are derived from the nonuniform gust loading.

Nomenclature

$\bar{A}$ = normalized root-mean-square response
$[H_{rg}]$ = frequency response matrix
$[I_e]$ = diagonal editor matrix
$[K_r]$ = covariance matrix
$K_{x/y}$ = modified spherical Bessel function of the third kind of order x/y
L = gust scale of turbulence
N_0 = mean frequency of zero crossings
$[PHF2]$ = MSC/NASTRAN generalized gust force matrix
$p(x, y)$ = bivariate Gaussian probability density function
$[QHJL]$ = MSC/NASTRAN force-downwash influence coefficient matrix
$\bar{q}$ = dynamic pressure
S = gust correlation strip separation distance
V = velocity
$[w_g]$ = gust downwash matrix
Γ = gamma function
γ_{ij} = cross-correlation coefficient between responses i and j
ν = reduced frequency, $\omega L/V$
σ = dimensionless spanwise separation distance, S/L
σ_w = gust root-mean-square velocity
$[\phi_g]$ = gust cross-spectral density matrix
$[\phi_r]$ = response cross-spectral density matrix
ω = circular frequency

Introduction

DESIGN load requirements for random gusts[1,2] prescribe one-dimensional gust fields, i.e., fields that are uniform spanwise for a vertical gust and uniform in the vertical direction for a lateral gust. The variation in the lateral and vertical gust velocities is only accounted for along the longitudinal axis, and the aircraft response to the lateral and vertical gust are treated independently. By definition, the vertical gust will produce a symmetrical vehicle response with corresponding symmetrical stresses, and the lateral gust will produce an antisymmetrical response with corresponding antisymmetrical stresses. Criteria for defining the corresponding design loads utilize these gust response characteristics in conjunction with specified turbulence field parameters, limit load exceedance requirements, and factors applied to the root-mean-square (rms) responses to arrive at "limit" loads. Most of these criteria are based upon studies of successful aircraft that relied on one-dimensional analysis techniques for deriving the appropriate requirements.[3,4]

The more general case of a three-dimensional gust will cause an asymmetric response, i.e., a combination of symmetric and antisymmetric responses. The one-dimensional assumption (spanwise uniformity for the vertical gust) can be unconservative, as exemplified by the fact that at the centerline of a flying wing symmetric shear and torsion are zero, whereas, the asymmetric values are not. This concern is not new and has been expressed in Refs. 5–9. Therefore, the problem is to determine how much coupling exists between the symmetric and antisymmetric responses of the vehicle for the general three-dimensional case.

Eichenbaum[9] has presented comparisons between one-dimensional and three-dimensional analyses for the C-5A aircraft. The results showed a decrease in loading on the wing while there was a small increase on the horizontal stabilizer. These results were explained by the effects of spanwise-averaging on the symmetric responses and the relative contributions of the antisymmetric responses to the overall loads on the components. These results were verified in part by comparison to flight test data which showed that the three-dimensional results compared much better to test data than did the one-dimensional results when assuming the von Kármán turbulence model.

Hoblit[10] has summarized comparisons of one-dimensional and three-dimensional analyses performed on the L-1011 aircraft. The results generally showed that the effect of the three-dimensional analysis is to reduce wing shear and bending moment responses. However, significant increases in wing torsion inboard of the engine were noted due to excitation of the first antisymmetric bending mode by the spanwise variation of gust velocity.

Johnston[11] compared measured L-1011 aircraft response to turbulence with both uniform and nonuniform gust analyses. These comparisons indicated that the nonuniform gust model more closely matched measured data than did the uniform gust model.

The USAF/Northrop B-2, because of its low wing loading and requirement to fly low-altitude terrain-following missions, includes one-dimensional gust conditions in its design set of

Presented as Paper 91-1048 at the AIAA/ASME/ASCE/AHS/ASC 32nd Structures, Structural Dynamics, and Materials Conference, Baltimore, MD, April 8–10, 1991; received April 8, 1991; revision received July 12, 1992; accepted for publication July 21, 1992. Copyright © 1991 by the American Institute of Aeronautics and Astronautics, Inc. All rights reserved.

*Engineer, Structural Dynamics Department, 8900 East Washington Boulevard.
†Manager, Loads Department, 8900 East Washington Boulevard. Member AIAA.
‡Consultant, 8900 East Washington Boulevard. Fellow AIAA.

load conditions. The B-2 also includes a very aggressive flight control system which is designed to provide significant improvements in ride quality and load alleviation during low-level contour flying. The one-dimensional vertical gust model is the basis for designing this aspect of the system and results in pitch axis control due to feedback of pitch axis response parameters measured along the centerline of the aircraft.

The primary purpose of this study was to assess the effects of nonuniform spanwise variations in vertical gust velocity on the B-2 gust response characteristics and determine if the nonuniform spanwise gust model would produce additional design load conditions. An additional area of interest was the effect on control system performance as exhibited in the computed loads.

The B-2 is sufficiently small in the vertical dimension that it can be considered planar, and the lack of vertical surfaces, nacelles, or external stores greatly reduces its sensitivity to lateral gusts. Furthermore, only the two-dimensional characteristics of the three-dimensional gust need be considered here.

Theoretical Development

The random response of a linear system to multiple random inputs has been given by Bendat and Piersol[12] and may be written as

$$[\phi_r(\omega)] = [H_{rg}^*(\omega)][\phi_g(\omega)][H_{rg}(\omega)]^T \tag{1}$$

where $[\phi_g(\omega)]$ is the cross-spectral density matrix of the random loadings at some frequency ω, $[H_{rg}(\omega)]$ is the frequency response matrix for each response caused by each of the harmonic loads at the frequency ω, and $[\phi_r(\omega)]$ is the cross-spectral density matrix of the various responses. This equation is general and may be applied to compute the response of an aircraft encountering a three-dimensional gust field.

The turbulence description for a three-dimensional gust is provided by the cross-correlation function of the statistically stationary, random, isotropic field of turbulence. This function can then be used to compute the cross-spectrum between gusts impinging upon any two points of the aircraft.

The cross-spectral density matrix for the Dryden and von Kármán forms have been derived for the three-dimensional case by Eichenbaum.[7-9] The von Kármán form is the turbulence model normally specified for gust loads analyses. For the present study we utilize the computational form presented by Houbolt and Sen,[13] which is

$$\phi_{12}(\nu) = \sigma_w^2[2^{2/3}/\Gamma(\tfrac{1}{3})](1/\sqrt{2\pi})(1/1.339)^{8/3}$$
$$\times [\tfrac{8}{3}(1.339)^2(\sigma^{5/3}/z^{5/6})K_{5/6}(z) - (\sigma^{11/3}/z^{11/6})K_{11/6}(z)] \tag{2a}$$

where $z = (\sigma/1.339) \times [1 + (1.339\nu)^2]^{1/2}$. The K are the modified spherical Bessel functions of the third kind tabulated by Abramowicz and Stegun.[14] The Bessel functions are obtained from the IMSL, Inc., Special Function Library subroutine DBSKS (XNU, X, N, BK) that calculates a sequence of N-modified Bessel functions of the third kind of order XNU for argument X. Equation (2a) reduces to

$$\phi_{12}(\nu) = \sigma_w^2 \frac{\sigma^{5/3}}{z^{5/6}}[0.518903K_{5/6} - 0.1085345(\sigma^2/z)K_{11/6}] \tag{2b}$$

A plot of the Von Kármán cross-spectral density evaluated by Eq. (2b) is shown in Fig. 1.

For the two-dimensional gust field, the subsonic aerodynamic loads may be obtained from the doublet-lattice method[15,16] by dividing the wing into strips (called gust correlation strips in this article) and considering the flow disturbance to be a harmonic gust traversing one strip at a time. The responses to the gust on one strip provide the elements

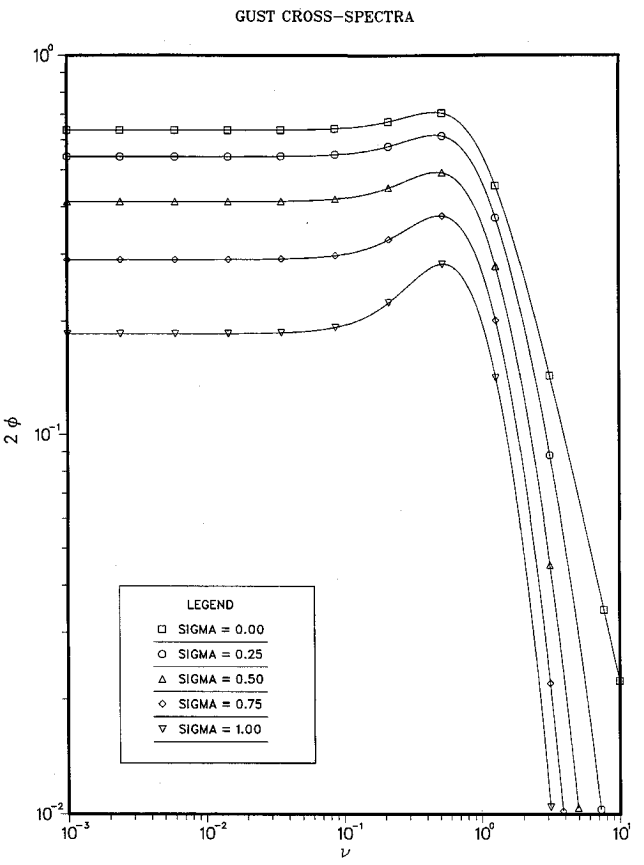

Fig. 1 Gust cross spectra for various values of $\sigma = S/L$.

of a single column of $[H_{rg}(\omega)]$; the responses to the gusts on all of the strips provide all of the columns of the matrix. The calculation of the frequency responses $[H_{rg}(\omega)]$ for a gust on each correlation strip has been carried out in MSC/NASTRAN which requires a user input solution sequence since the basic NASTRAN gust frequency response assumes a uniform one-dimensional gust. The GUST module computes generalized gust forces from

$$[PHF2] = \bar{q}[QHJL][w_g] \tag{3}$$

where $[w_g]$ is the matrix of gust downwashes at the $\frac{3}{4}$-chord location of each aerodynamic box induced by the one-dimensional harmonic gust field. To compute the downwash due to a gust acting on a single strip $[w_g]_s$, we introduce an editor matrix to modify the uniform gust field downwashes $[w_g]$

$$[w_g]_s = [I_e]_s[w_g] \tag{4}$$

where $[I_e]_s$ is a diagonal matrix whose elements are unity for all boxes on the correlation strip under consideration, and zero elsewhere. The matrix $[w_g]$ is not accessible since it is computed internally in the GUST module, but $[QHJL]$ can be modified through postmultiplication by $[I_e]_s$ in order to obtain the desired result:

$$[PHF2]_s = \bar{q}[QHJL][I_e]_s[w_g] \tag{5}$$

Once the cross-spectral matrix for the response, Eq. (1), has been obtained for all the frequencies of interest at a specified flight condition and gust scale of turbulence, numerical integrations are performed up to the cutoff frequency in order to obtain the statistical parameters of interest. Those parameters are $\bar{A}$, N_0, γ_{ij}, and the probability density distribution functions of the assumed Gaussian random process.

The $[K_r]$ of the response is found by integrating the cross-spectral density matrix up to the cutoff frequency Ω_c:

$$[K_r] = \left(\frac{1}{2\pi}\right) \int_0^{\Omega_c} [\phi_r(\omega)]\, d\omega \tag{6}$$

The integrals are numerically evaluated using the trapezoidal rule. The rms responses are found from the diagonal elements of Eq. (6):

$$\sigma_i = \sqrt{K_{ii}} \tag{7a}$$

$$= \sigma_g \bar{A} \tag{7b}$$

The mean frequency of zero crossings is found from

$$N_0^2 = \left(\frac{1}{2\pi\sigma_i^2}\right) \int_0^{\Omega_c} \omega^2 \phi_{ii}(\omega)\, d\omega \tag{8}$$

and the trapezoidal rule is again used to perform the numerical integration.

The cross-correlation coefficient between two responses is

$$\gamma_{ij} = (K_{ij}/\sigma_i\sigma_j) \tag{9a}$$

or

$$\gamma_{ij} = (K_{ij}/\sqrt{K_{ii}K_{jj}}) \tag{9b}$$

Probability data are the last requirement. If we assume that atmospheric turbulence is a stationary Gaussian random process, the response will also be a stationary Gaussian random process since we have modeled a linear system. For two responses, x and y, the bivariate Gaussian probability density distribution function is

$$p(x, y) = \frac{1}{2\pi A_x A_y \sqrt{1 - \gamma_{xy}^2}} \exp\left[\frac{-1}{2(1 - \gamma_{xy}^2)} \times \left(\frac{x^2}{A_x^2} - \frac{2\gamma_{xy}xy}{\overline{A_x}\,\overline{A_y}} + \frac{y^2}{A_y^2}\right)\right] \tag{10}$$

To compare the two-dimensional gust field response probability characteristics with those of the one-dimensional gust, we consider the equal probability combination of x and y, for which the constant probability density distribution is

$$p_\sigma(x, y) = [1/2\pi A_x A_y \sqrt{e(1 - \gamma_{xy}^2)}] \tag{11}$$

and the equation that describes the constant probability elliptical boundary is

$$(x^2/A_x^2) - (2\gamma_{xy}xy/\overline{A_x}\,\overline{A_y}) + (y^2/A_y^2) = 1 - \gamma_{xy}^2 \tag{12}$$

The probability characteristics of the one- and two-dimensional gusts may be compared by superimposing the corresponding ellipses.

B-2 Basic Modeling

All modeling and basic frequency response calculations for the present analyses are carried out in MSC/NASTRAN. The basic model consists of a full-span idealization which is composed of three constituent parts: 1) structural, 2) aerodynamic, and 3) control system models. A general overview of the modeling is described below.

The B-2 is structurally modeled by a finite-element model (FEM) which has been developed for dynamics analysis. The inertia distribution is prescribed by a distributed lumped mass model using the NASTRAN CONM2 features. Three weight configurations were considered in this study: 1) light, 2) medium, and 3) heavy. The weight configurations reflect the addition of fuel from inboard to outboard locations along the span. Figure 2 summarizes natural frequencies and shows normal mode shapes for the three weight configurations. Plunge, pitch, and roll rigid body degrees of freedom (DOF) were also included in the model.

The aerodynamic model, Fig. 3, consists of a full-span 628-box doublet-lattice idealization developed for this study. Also indicated on the figure is the definition of each of the 15 gust

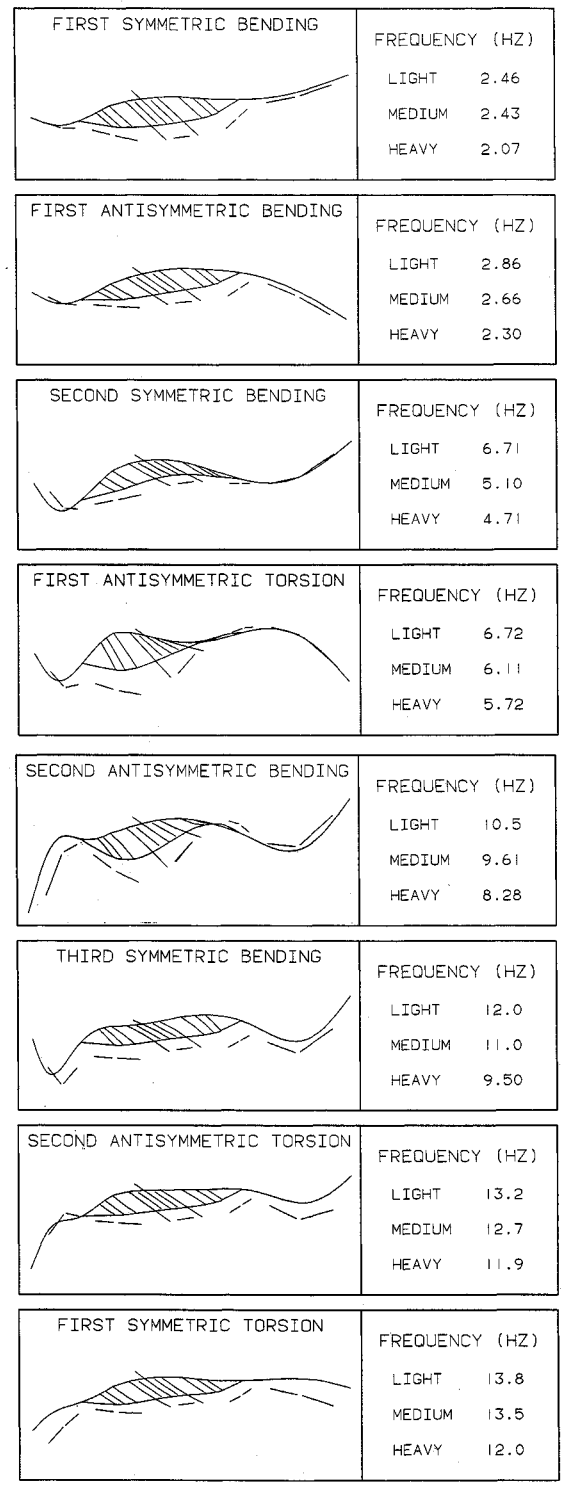

Fig. 2 Mode shapes and frequencies.

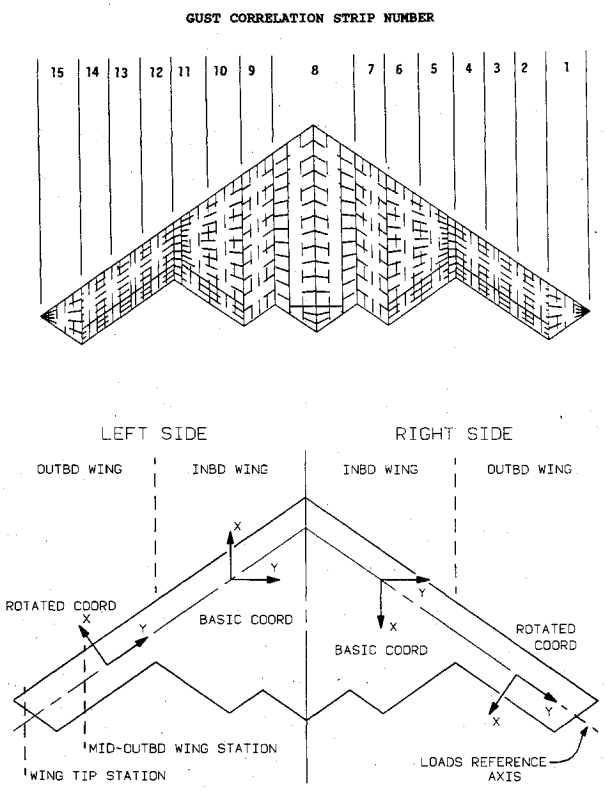

Fig. 3 Aerodynamic model with correlation strips and loads coordinate system.

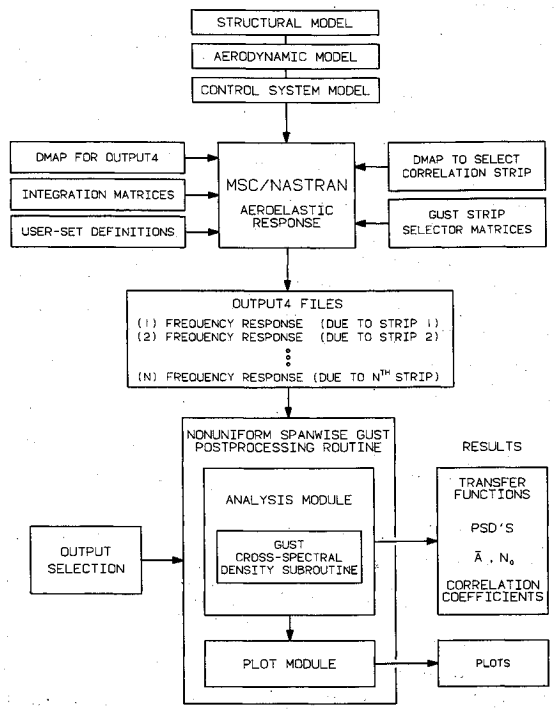

Fig. 4 Solution sequence flow chart.

"correlation" strips used for developing the spanwise strip loading.

The B-2 flight control system is a state of the art fly-by-wire system with performance requirements which include ride quality and load alleviation functions during low-altitude terrain-following operations. Key elements of this system have been included in the present analyses, including modeling of sensor elements, control surface actuators, and the relevant closed loop control laws. Control is achieved through actuation of trailing-edge control surfaces consisting of a center body device and elevons distributed across the span. Only the pitch axis active control system model has been included in the current study. Flight control system parameters were fixed for all of the analyses reported herein.

Airframe loads (shear, bending moment, and torque) are calculated using load integration matrices which operate on grid point forces generated from the stiffness matrix and the computed deflections. This calculation is performed in the frequency domain, thus assuring the correct phasing of the forces in the integrations. Figure 3 shows the integrated loads coordinate system and indicates spanwise locations where responses are compared in the results section. Basic coordinate system loads are used when comparing loads on the inboard wing, and the rotated loads are used for the outboard wing.

Solution Procedures

The nonuniform gust solution procedure developed for this study is comprised of two individual routines. The first routine performs aeroelastic response calculations using the finite-element structural, aerodynamic, and control system models previously described. The second routine processes the frequency response data by means of a series of FORTRAN programs which compute the gust response parameters as defined by the equations defined earlier. This sequence is shown schematically in Fig. 4.

The aeroelastic response calculations are performed using MSC/NASTRAN Solution 76 in conjunction with two user input programs denoted as Direct Matrix Abstraction Programs (DMAP). The first DMAP performs the matrix algebra necessary to produce integrated shear, moment, and torque load data. This DMAP also ensures that all required data are output to FORTRAN-readable files (NASTRAN OUTPUT4 files).

The second DMAP selects the correlation strip over which the gust is to be applied. This is accomplished by using the editor matrix to select the appropriate downwash terms as described above in the theoretical development section. The frequency response of the system is then computed separately for each of the gust correlation strips.

As indicated on Fig. 4, the FORTRAN postprocessing routine computes the gust cross-spectral density matrix, power spectral density (PSD), rms values, frequency of zero crossing, and cross-correlation coefficient data. All plotting is also performed in this routine.

Results

Results have been developed for a single flight condition, high speed (subsonic) at sea level, and three weight conditions: 1) light, 2) medium, and 3) heavy. Two scales of turbulence were considered: 1) $L = 500$ ft and 2) $L = 2500$ ft. Key elements of the analyses are shown for selected response parameters. These include PSDs, $\bar{A}$ and N_0, integrated spanwise loading, and combined load envelopes. All results are compared to the uniform gust input.

PSD and ($\bar{A}$)

PSDs of centerline bending moment are presented in Figs. 5–8. $\bar{A}$ and N_0 comparisons are tabulated on the figure. Selected results for two weight conditions are presented. Two scales of turbulence are shown for the lightweight condition.

Figure 5 shows results for the lightweight condition for $L = 500$ ft, which indicates that the uniform gust produces more power over the entire frequency range except at low frequency. $\bar{A}$ is higher for the uniform gust. Figure 6 shows results for a $L = 2500$. Response levels are generally lower than for $L = 500$, as would be expected; however, the fractional differences between the uniform and nonuniform $\bar{A}$ are little changed, indicating that L is not a significant parameter for the range of L considered.

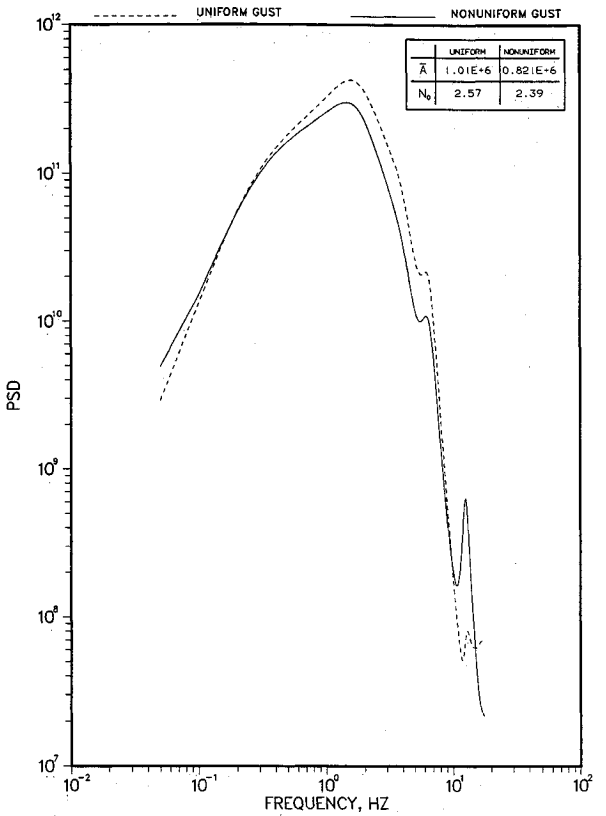

Fig. 5 PSD of basic-axis centerline wing bending moment (lightweight case, small scale of turbulence).

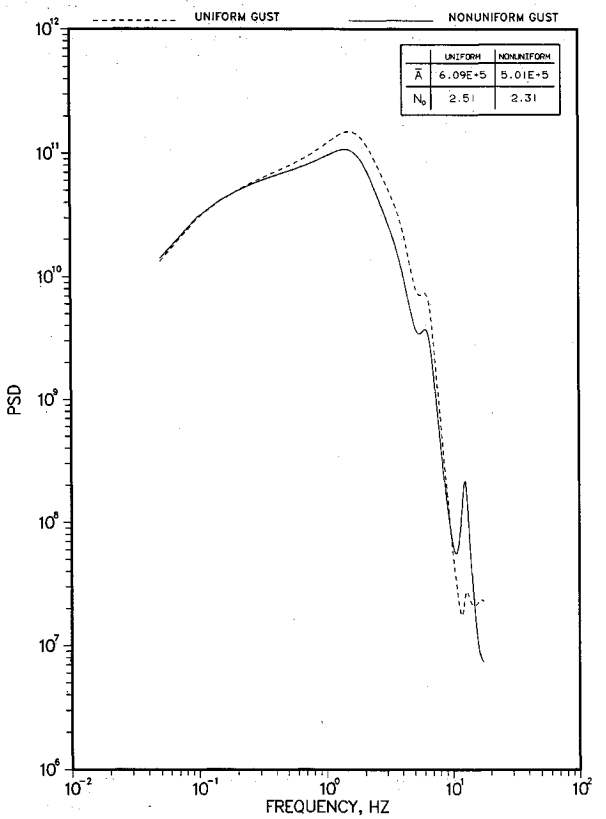

Fig. 6 PSD of basic-axis centerline wing bending moment (lightweight case, large scale of turbulence).

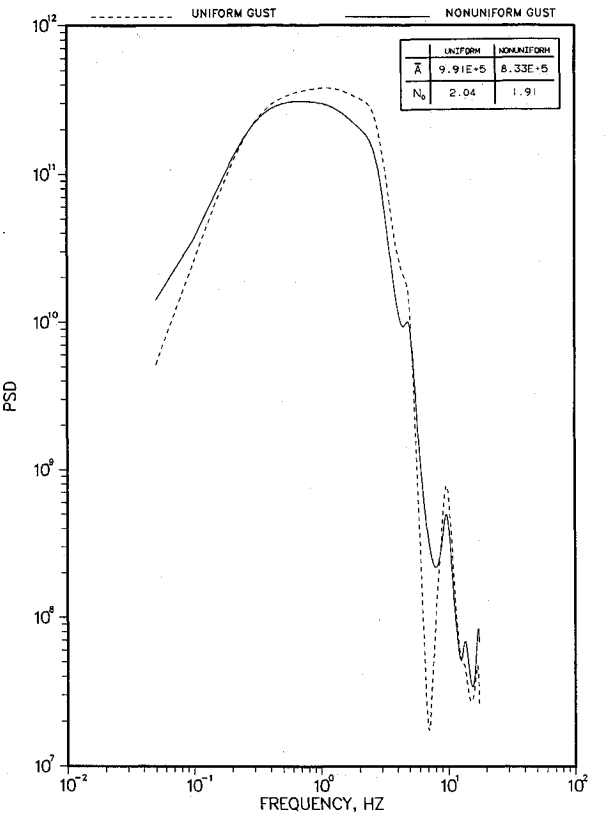

Fig. 7 PSD of basic-axis centerline wing bending moment (heavyweight case, small scale of turbulence).

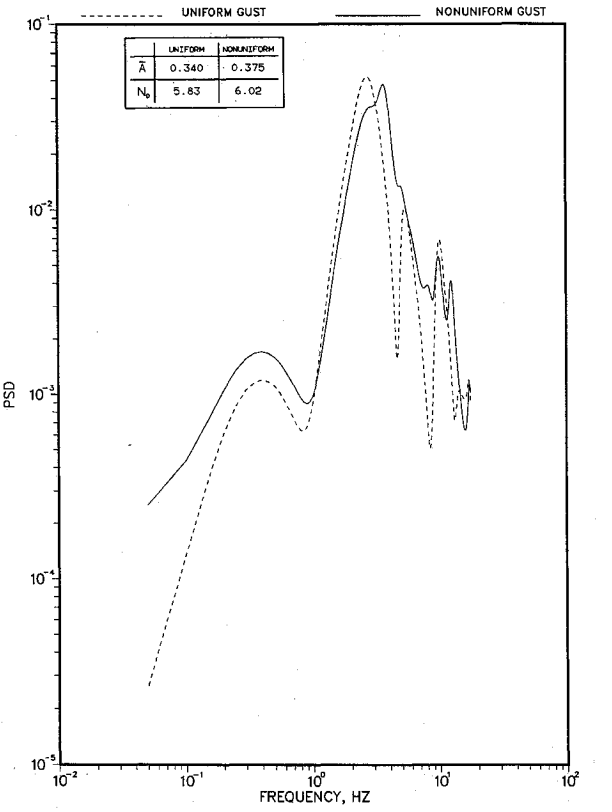

Fig. 8 PSD of wing tip acceleration (heavyweight case, small scale of turbulence).

Figure 7 shows PSD results for the heavyweight condition. Results generally indicate that the uniform gust responses are larger than the nonuniform responses; however, there is some sensitivity to weight distribution.

Table 1 compares $\bar{A}$ values for several response parameters for each of the three weights. For the heavyweight condition, the uniform and nonuniform results are closer in magnitude. The wing tip acceleration response is larger for the nonuniform gust. These results can be explained by the decrease in frequency of the antisymmetric modes into the bandwidth of the gust PSD. The antisymmetric modes are not contributors during the symmetric response to the uniform gust, but are

Table 1 Comparison of $\bar{A}$ response

Weight condition	c.g. Acceleration, g			Wing tip acceleration, g			Outboard wing bending moment, 10^4 in.-lb		
	U[a]	NU[b]	U/NU[c]	U	NU	U/NU	U	NU	U/NU
Light	0.078	0.065	1.19	0.778	0.641	1.21	8.53	7.40	1.15
Medium	0.069	0.059	1.17	0.520	0.540	0.960	7.67	7.46	1.03
Heavy	0.067	0.061	1.09	0.340	0.375	0.910	8.44	8.02	1.05

[a]Uniform gust response. [b]Nonuniform gust response. [c]Ratio of uniform-to-nonuniform gust response.

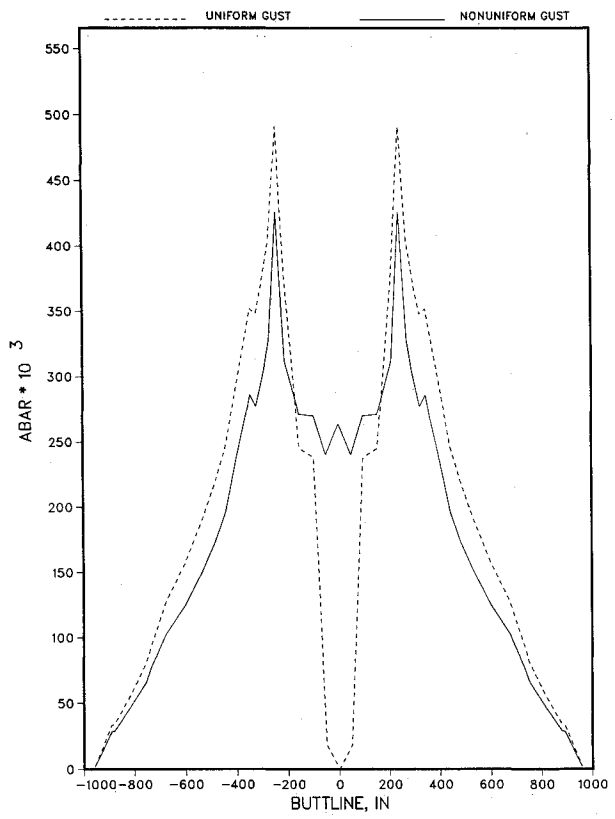

Fig. 9 Spanwise load distribution of rms basic-axis torsion (lightweight case, small scale of turbulence).

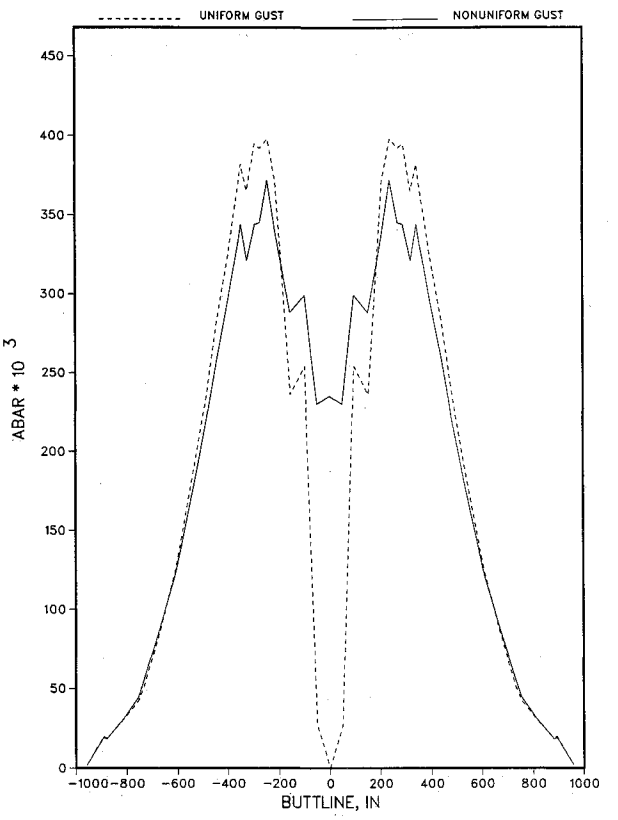

Fig. 10 Spanwise load distribution of rms basic-axis torsion (heavyweight case, small scale of turbulence).

additional contributors during the asymmetric response to the nonuniform spanwise gust. This is clearly seen in the PSD of the wing tip acceleration response of Fig. 8.

It should be noted that comparison of rms response between the uniform and nonuniform gust does not neccessarily indicate the difference in design load levels predicted between the two gust models. As indicated in the Introduction, design limit loads are determined from rms response in combination with specified scaling parameters and frequency of exceedance requirements. Existing requirements are only applicable to the uniform gust model. Hoblit[10] provides a good discussion of this.

Characteristic frequency N_0 values are compared for each response; however, no conclusions are drawn here because the cutoff frequency used in the integration was not a study parameter.

Spanwise Load Integrations

Spanwise integrated $\bar{A}$ for bending moment and torsion are presented in Figs. 9–12. Selected results are shown for two gross weights. Only L = 500 ft is considered here.

Figures 9 and 10 show integrated torsion in the basic coordinate system for the light- and heavyweight conditions, respectively. The most striking feature is the nonzero value at the centerline for the nonuniform spanwise gust case. The uniform gust solution must be zero at the centerline of a flying wing configuration because of load equilibrium requirements. Outboard of BL 150, the uniform gust response generally produces the higher loads, although there is some sensitivity to weight conditions as seen in Fig. 10.

Figures 11 and 12 show integrated bending moment in the basic coordinate system for the light- and heavyweight conditions. The uniform gust produces higher loads over the entire span for both conditions. There is a general trend of lower loads inboard and higher loads outboard with increasing weight due to inertia effects associated with fuel distribution.

Combined Load Envelopes

Combined load envelopes defined from equal probability considerations are discussed above in the theoretical section. The equal probability envelope indicates the degree of correlation between response parameters. If the correlation coefficient is equal to one, implying total correlation, the ellipse collapses to a straight line along the major axis. If it is equal to zero, implying no correlation, the ellipse degenerates into a circle. Figures 13 and 14 show representative envelopes for bending/torsion at the midoutboard wing station for the light- and heavyweight conditions.

For both cases, the nonuniform gust response shows less correlation between bending and torsion than the uniform gust response. Results also show that the nonuniform gust loads exceed the uniform gust loads along the minor axis of

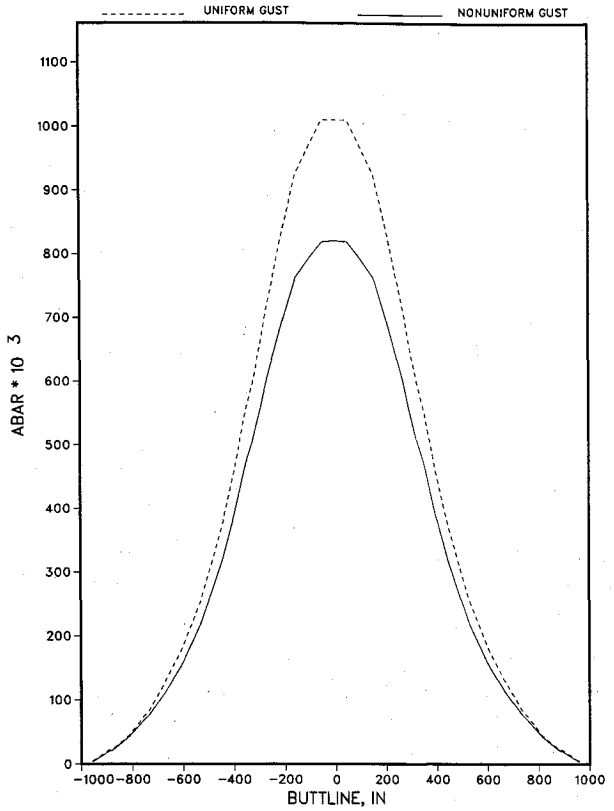

Fig. 11 Spanwise load distribution of rms basic-axis bending moment (lightweight case, small scale of turbulence).

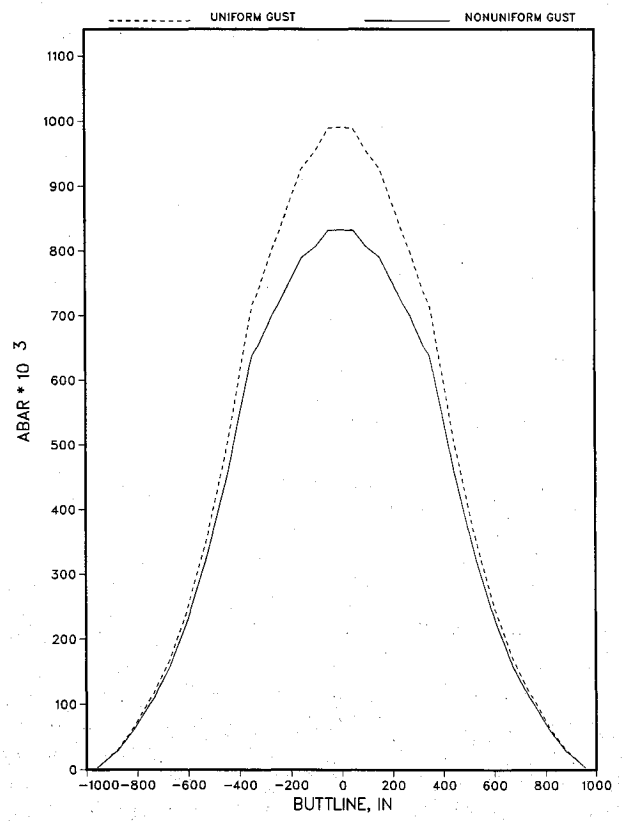

Fig. 12 Spanwise load distribution of rms basic-axis bending moment (heavyweight case, small scale of turbulence).

the ellipse for the heavier weight condition. This is true even though the individual bending and torsion $\bar{A}$ are smaller for the nonuniform gust and results from the more circular envelopes. This is not of practical concern, however, because maneuver conditions usually dominate in those corners of the envelope.

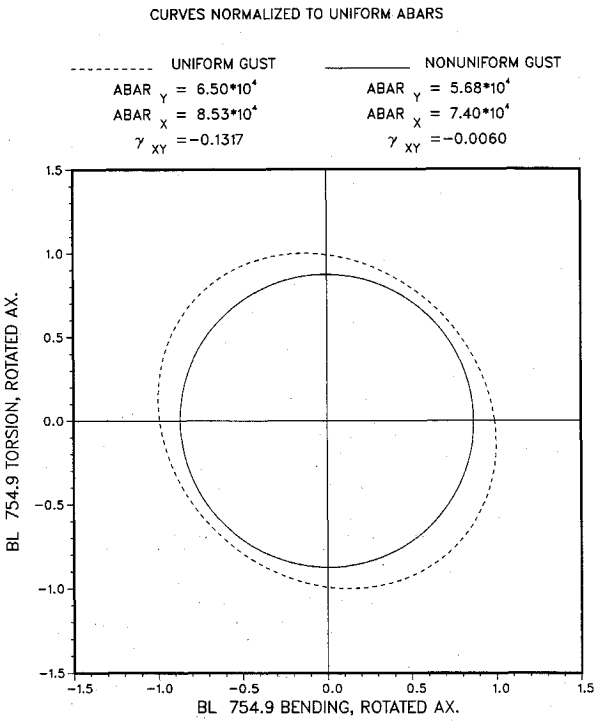

Fig. 13 Combined rotated-axis load diagram at midoutboard wing (lightweight case, small scale of turbulence).

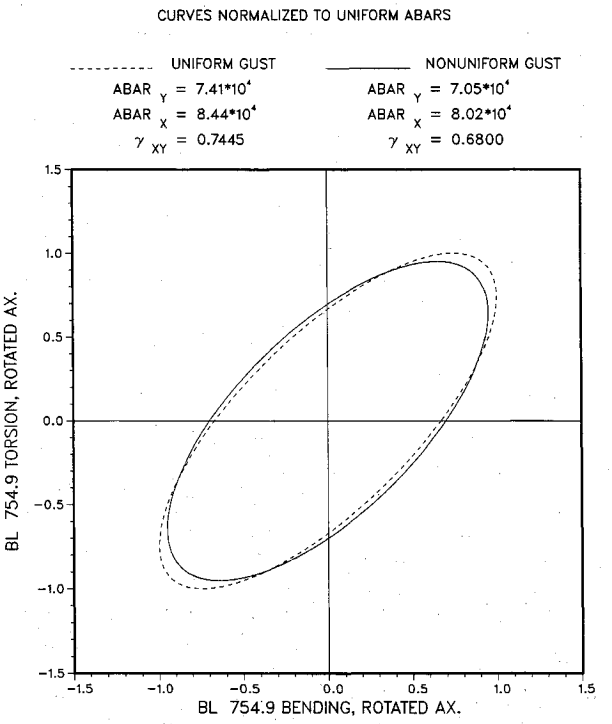

Fig. 14 Combined rotated-axis load diagram at midoutboard wing. (heavyweight case, small scale of turbulence).

Concluding Remarks

The calculated results show that, in general, the nonuniform gust model produces lower rms acceleration response and airframe loading than the uniform gust model. Near the centerline the nonuniform gust model produced higher loads for shear and torque which, for the uniform gust, are identically zero because of load equilibrium requirements. These higher loads are not of concern in strength considerations because the critical conditions result from maneuvering and ground load conditions. However, these gust loads could provide design conditions for fatigue considerations.

Outboard wing loads for the nonuniform gust model were generally lower than for the uniform model. The combined load envelopes for the mid- and heavyweight conditions produced by the nonuniform model did penetrate the uniform gust envelopes about the minor axis of the ellipse. This occurs because of small differences in the $\bar{A}$ responses between the two models and the correlation characteristics of the nonuniform gust. These load envelope points are not of concern because roll maneuver design conditions usually dominate those corners of the load envelope.

It can be concluded from the results that there is no adverse coupling between the nonuniform gust loading and the flight control system. Although airframe loads were generally lower for the nonuniform gust loading than for the uniform gust case, specific control system performance parameters were not evaluated. Unpublished results by the authors for an open-loop flight control system configuration show similar comparisons, on a fractional basis, between the uniform and nonuniform gust loads, as reported here for the closed-loop case.

It is the opinion of the authors that these results are not unexpected for the B-2 flying-wing configuration. The symmetric response is reduced because of the nonuniformity of the gust across the span, and the power in the turbulence has decreased significantly at the first flexible antisymmetric wing bending frequency, resulting in an overall rms response which is less than that for the uniform gust response. Configurations with vertical surfaces, external stores, or low frequency antisymmetric structural modes (relative to corresponding symmetric modes) such as a T-tail configuration, may not show similar results.

Current design criteria defined in FAA regulations and Military Specifications prescribe analyses based on the uniform-gust model and define design load requirements in terms of those results. It is, therefore, not possible to utilize nonuniform gust analysis results for developing design load requirements until such time as suitable criteria are available. In the meantime, nonuniform-gust analysis methods will continue to be useful for providing analysis results for correlating with in-flight measured gust response data.

References

[1]Military Specification, "Airplane Strength and Rigidity, Flight Loads," MIL-A-008861A (USAF), March 1971.

[2]Federal Aviation Regulation, "Part 25—Airworthiness Standards: Transport Category Airplanes," Code of Federal Regulations, Title 14, *Aeronautics and Space*, Sept. 1980.

[3]Austin, W. H., "Development of Improved Gust Load Criteria for United States Air Force Aircraft," Aeronautical Systems Div., Air Force Systems Command, Systems Engineering Group TN-67-28, Wright-Patterson AFB, OH, Sept. 1967.

[4]Turner, E. W., "An Exposition on Aircraft Response to Atmospheric Turbulence Using Power Spectral Density Analysis Techniques," Air Force Flight Dynamics Lab. TR-76-162, Wright-Patterson AFB, OH, May 1977.

[5]Houbolt, J. C., "On the Response of Structures Having Multiple Random Inputs," Jahrbuch 1957 der WGL, Friedr. Vieweg and Sohn, Braunschweig, Germany, pp. 296–305.

[6]Fuller, J. R., "A Procedure for Evaluating the Spacewise Variations of Continuous Turbulence on Airplane Response," *Journal of Aircraft*, Vol. 5, Jan.–Feb. 1968, pp. 49–52.

[7]Eichenbaum, F. D., "A New Method for Computing the Dynamic Response of Aircraft to Three-Dimensional Turbulence," *Proceedings of AIAA Structural Dynamics and Aeroelasticity Specialist Conference*, Orlando, FL, April 16–17, 1969, pp. 84–94.

[8]Eichenbaum, F. D., "Response of Aircraft to Three Dimensional Random Turbulence," Air Force Flight Dynamics Lab. TR-72-28, Wright-Patterson AFB, OH, Oct. 1972.

[9]Eichenbaum, F. D., "Evaluation of Three-Dimensional Turbulence Techniques," Air Force Flight Dynamics Lab. TR-74-151, Wright-Patterson AFB, OH, March 1975.

[10]Hoblit, F. M., "Gust Loads on Aircraft: Concepts and Applications," AIAA Education Series, Washington DC, 1988, pp. 165–167.

[11]Johnston, J. F., et al., "Evaluation of Accelerated Development and Flight Evaluation of Active Controls Concepts for Subsonic Transport Aircraft, Volume 1—Load Alleviation/Extended Span Development and Flight Test," NASA CR-159097, Sept. 1979.

[12]Bendat, J. S., and Piersol, A. G., *Measurement and Analysis of Random Data*, Wiley, New York, 1966.

[13]Houbolt, J. C., and Sen, A., "Cross-Spectral Functions Based on von Kármán's Spectral Equation," NASA CR-2011, March 1972.

[14]Abramowicz, M., and Stegun, I. A., *Handbook of Mathematical Functions with Formulas, Graphs, and Mathematical Tables*, National Bureau of Standards, Applied Mathematics Series, No. 55, June 1964.

[15]Albano, E., and Rodden, W. P., "A Doublet Lattice Method for Calculating Lift Distributions on Oscillating Surfaces in Subsonic Flow," *AIAA Journal*, Vol. 7, No. 2, pp. 279–285; see also No. 11, 1969, p. 2169.

[16]Giesing, J. P., Rodden, W. P., and Stahl, B., "Sears Function and Lifting Surface Theory for Harmonic Gust Fields," *Journal of Aircraft*, Vol. 7, No. 3, 1970, pp. 252–255.